C.P. No. 1255

MINISTRY OF DEFENCE (PROCUREMENT EXECUTIVE)

AERONAUTICAL RESEARCH COUNCIL

CURRENT PAPERS

Rotating Stall and Casing Wall Boundary Layers in an Axial Flow Compressor

By

C. Lakhwani,

Department of Engineering,

University of Cambridge

Communicated by Prof. J. H. Horlock

LONDON: HER MAJESTY'S STATIONERY OFFICE

1973

PRICE 35p NET

*C.P. No.1255
July, 1972

ROTATING STALL AND CASING WALL BOUNDARY LAYERS IN AN AXIAL FLOW COMPRESSOR

- by -
C. Lakhwani,
Department of Engineering,
University of Cambridge

SUMMARY

An experimental investigation has been made to study the effect of casing wall boundary layers upon the rotating stall characteristics of an axial flow compressor in an isolated rotor row configuration. The boundary layer was modified by fixing circular rings of different wire diameters to the outer casing. A significant alteration of the rotating stall characteristics was obtained with regard to changes in flow coefficient at stall onset and cessation.

---

*Replaces A.R.C.33 898

1. Introduction

In most compressors and experimental test-rigs it has been observed that stall onset occurs at either the hub or the tip section. This suggests that it might be an effect related to wall boundary layers. This possibility has been accepted by some investigators but it is argued that understanding of wall boundary layers in turbomachines is not sufficiently advanced to warrant a detailed approach. Although this may be true for a complete theoretical analysis, in particular for the case of turbulent boundary layers, a careful experimental investigation should indicate any coupling between the mechanism of stall and annulus wall boundary layers. The experiments described below are part of such an experimental study.

The outer casing wall boundary layer at entry to an axial flow compressor was modified by fixing circular wires of different sizes on to the casing, upstream of an isolated rotor blade row. The resulting effects on the stall inception and stall cessation characteristics were investigated.

2. Apparatus and Experimental Method

2.1 Preliminary tests to determine the influence of circular wires on wall boundary layers

In order to find the effect of circular wires on the boundary layer on the compressor annulus wall, preliminary tests were performed in a wind tunnel with straight side walls. The working section of the tunnel was 18 in × 26 in and wires about 24 in long were fixed to one wall. Velocity profiles were obtained at stations 1, 5 and 10 in downstream of the position where the wires were fixed. Six different sizes of circular wires were tested (Table 1). A constant temperature DISA 55A01 hot-wire anemometer was used. The velocity of the air in the tunnel was in the same range as the velocity for the tests in the axial flow compressor.

Wire No.	Wire Dia. (in)
1	0.019
2	0.036
3	0.065
4	0.105
5	0.141
6	0.192

Table 1

The two smallest diameter wires did not modify substantially the velocity profile. For the other cases, the influence of the wire had decayed at the stations 5 and 10 in downstream. It was therefore decided to neglect the two small sizes and use three of the other sizes; and to place them 2.45 in upstream of the compressor rotor tip.

2.2/

2.2 The axial flow compressor

The axial flow compressor rig used is illustrated in Fig.1. The compressor is driven by a 25 HP induction motor by a step-up gear box; the available gear ratios being 2.086:1 and 1.536:1. The motor rotates at a speed of approximately 2900 RPM. For all the experiments described below the gear ratio used was 1.536:1.

The air is drawn through an annular airmeter, covered by an entry gauze, and flows past four inlet webs before passing into the compressor and then into a conical diffuser. An exit throttle controls the air flow. The compressor may be built in five rows, to give two complete stages, and either of the moving rows and any one or all of the stationary rows may be removed. A row of outlet straightening vanes is located before the diffuser. The hub-tip ratio is constant through the compressor and equals 0.40 (r_{hub} = 2.8 in r_{tip} = 7 in). In the present tests, the compressor was assembled in an isolated rotor row configuration, Fig.2.

The entry airmeter had been previously calibrated, Horlock[1], by traversing a pitot-tube across the entry on plane 1. A flow coefficient was obtained, enabling a plot of $(\frac{Q\sqrt{T}}{B})$ against $(h/_B)$ to be made. The mass flow rate was obtained by measuring the mean depression, $\underline{h}$, on plane 1 of the airmeter and using the above mentioned calibration. The mean axial velocity in the compressor, $\overline{C}_x$, was calculated from knowledge of this mass flow and the cross sectional area of the annulus.

The blade speed, U_m, was calculated from the observed motor speed and knowledge of the gear ratio used.

2.3 The blading

The rotor blades used were cast reinforced plastic blades designed by Louis[2] and manufactured for him following a process developed by Horlock[3]. The design was that of a rotor of a free vortex stage; the number of blades was 19, constant 1.5 in chord. The blade stagger angle was 25° at the hub, the variation of $s/_c$ and the blade angles are given in Fig.3.

2.4 The circular wire rings

Following the preliminary tests, three different sizes of wires were used: 0.065, 0.125 and 0.189 in diameter. Circular rods and wires were bent to the shape of rings to fit the inner part of the casing.

In the cases of the two larger wire diameter rings, holes were drilled and tapped in the rings so that these could be secured to the annulus wall by means of screws through existing pressure tappings on the casing, Fig.3. The smallest wire diameter ring was fixed to the casing wall by means of an epoxy resin.

2.5 Instrumentation

Velocity profiles upstream of the rotor, prior to stall, were obtained by traversing radially a 3-hole cylindrical probe which had been previously calibrated against an NPL type probe in a calibration duct. In the proximity of the casing wall region, a pitot-tube in conjunction with readings from wall

pressure tappings was used. Both these probes were accommodated in a traversing gear, readings being accurate to within 0.025 in.

For the non-dimensional characteristics, the mean stagnation pressure rise coefficient was obtained by area averaging readings from traverses obtained both upstream and downstream of the rotor (positions P_3 and P_4 respectively).

The shape and patterns of the stall cells were obtained using two hot wire probes downstream of the rotor. One of these was kept fixed as reference near the casing wall and the other was traversed radially. These probes were connected to a constant current battery operated anemometer. Traces were obtained on U.V. recording paper in a Southern Instruments recorder, using high sensitivity $5KH_z$ liquid damped galvanometers, about 100 different recordings were made.

The position of the rings, probes and rotor are shown in Fig.2.

3. Experimental Results

3.1 Changes in characteristics with entry boundary layer thickness

Fig.4 shows the different axial velocity profiles upstream of the rotor obtained, just before the onset of stall, for the various types of circular-wire rings used. These profiles vary substantially and a gradual increase in the casing wall boundary layer displacement thickness (δ^*) is observed with increase of diameter of the wires used. To obtain the

displacement thickness $\left(\delta^* = \int_0^{\delta} \left(1 - \frac{C_x}{C_{x_{max}}}\right) dy\right)$, was taken as the

position where $C_x = C_{x_{max}}$, which corresponded to $\delta = 1.20$ in and this value was the same for all four cases.

The variation of the flow coefficients at stall onset and stall cessation with casing wall boundary layer displacement thickness is shown in Fig.5. This shows a substantial increase in the value of $\phi_{\text{stall onset}}$ with δ^*. The hysteresis effect between the stall onset and stall cessation flow coefficient is observed to decrease with δ^*.

Figs.6a, 6b show the non-dimensional total pressure rise

$\left(\frac{\Delta P_s}{\frac{1}{2}\rho U_m^2} \text{ vs. } \frac{\overline{C}_x}{U_m}\right)$ and the wall static pressure rise $\left(\frac{\Delta P_w}{\frac{1}{2}\rho U_m^2} \text{ vs. } \frac{\overline{C}_x}{U_m}\right)$

characteristics for the compressor rotor with a plain casing and with a 0.189 in diameter at entry. These show a substantial deterioration in total pressure rise at stall, with increasing δ^*, which narrows considerably the stall margin.

From the total pressure rise characteristics, it is seen that on increasing δ^* the stall appears to change from the abrupt type to a nearly progressive type stall.

3.2 Stall cells

In all four sets of tests, the compressor stalled abruptly with a distinctive change in the noise level. Observations of the stall cells from the U.V. traces showed that for the plain casing case, rotating stall inception

was/

was with one cell and, in most cases, this would split into two smaller cells rotating at the same speed as that of the initial cell. On cessation of stall, these two cells would recombine into one cell before coming out of stall. An interesting change in the stall patterns was observed when using the circular wire rings. No tendency to form a two-cell pattern was observed and in fact only once did the initial cell split into two smaller cells, the reverse happening on cessation. This was 1 in from the casing for the 0.065 in wire. Also, for the 0.125 in wire, on one occasion near the hub, stall inception was observed to occur with two cells but when this test was repeated stall onset was always with one single stall cell.

For tests on another experimental set-up[4], using a 5 ft diameter rotating cascade, the stall pattern obtained was throughout also that of a single cell. The boundary layer in this rig was of the order of $\delta = 1.50$ in (in the present investigation $\delta = 1.25$ in) and these results may indicate that for thick outer annulus boundary layers the tendency is to form a one large cell stall pattern.

Comparing the recordings at different radial positions, it was observed that near the tip region, in the condition of rotating stall, the stall cell had regions of velocity both higher and lower than the mean flow velocity just before stall, the regions of higher velocity quickly diminishing radially inwards. At about 1 in from the casing the stall-free region mean velocity was the same as that before stall and the velocity in the cells was very much lower, shown by pronounced peaks. Approaching closer towards the hub, the mean velocity increased substantially and the minimum velocity, corresponding to the stall cells, was equal to that of the unstalled flow velocity at the corresponding radius prior to stall onset. These results are diagrammatically summarised in Fig.7. These observations contradict the general belief that a stall cell is completely a region of velocity deficit.

The stall cells extended over about 25 to 40% of the annulus cross sectional area, the extent of the cells decreasing slightly as the boundary layer was thickened. As had been previously observed on a rotating cascade[4], the minimum extent of the cell occurred in the mid span region. On the compressor coming out of stall there was a decrease in the size of the cell with a relatively large region remaining stalled near the hub before complete disappearance of the stall cell.

The ratio of the stall speed to the mean blade speed was constant and the same for all four sets of tests. The value of this ratio being $0.56 \rightarrow 0.57$. This was calculated by obtaining the average over forty revolutions of the stall cells. This result seems to indicate that the stall cell speed is dependent on the geometry and configuration of the blade rows in a compressor and does not depend on the onset and cessation characteristics or on the boundary layer thickness. A similar effect had been observed on the large rotating cascade[4], where although the stall inception and cessation flow coefficient changed with Reynolds number in the low range, the ratio of stall cell speed to blade speed remained constant throughout. In the work reported in Ref.4, only when the number of blades in the isolated rotor row was changed, or when a stator blade row was added, did this ratio change.

Oscillations of the mean flow velocity were observed in the mid span region both before stall onset and after stall cessation, this latter effect being more pronounced.

Conclusions/

4. Conclusions

(1) Increasing the casing wall boundary layer displacement thickness brings about onset of stall at higher mass flow rates, decreases hysteresis effects and tends towards giving a progressive type stall.

(2) Stall patterns are changed when the boundary layer on the casing wall is modified.

(3) Regions of velocity both higher and lower than the mean stall-free velocity have been observed in stall cells.

(4) The ratio of stall cell speed to blade speed is not influenced by changes in the entry boundary layer thickness.

(5) As δ^* was increased the onset of stall occurred at higher flow rates. At high flow coefficients the upstream axial velocity is higher and the incidence lower in the mainstream, indicating that stall onset was determined by conditions in the wall boundary layer region and not by the incidence in the mainstream.

References/

References

No.	Author(s)	Title, etc.
1	J. H. Horlock.	Some aerodynamic problems of axial flow turbomachines. Ph.D. Thesis, CUED. 1955.
2	J. F. Louis	Stall phenomena in axial flow compressors. Ph.D. Thesis, CUED. 1957.
3	J. H. Horlock	The manufacture of glass cloth resin blades for an axial flow compressor. Journ. Roy. Aero. Soc. June, 1957.
4	C. Lakhwani and H. Marsh	Rotating stall in an isolated rotor row. I. Mech. Eng. Conference on 'Heat and fluid flow in steam and gas turbing plant'. 1973.

Notation/

Notation

B = Barometric pressure (lb/in^2)

C_x = Axial velocity

$\overline{C}_x$ = Mean axial velocity in compressor, calculated from knowledge of mass flow rate and annulus area.

ς = Mass flow rate (lb/sec)

T = Absolute inlet temperature (°K)

U_m = Blade speed at mean radius

c = Blade chord

h = airmeter static depression

l = Blade height

r = Radius

s = Blade pitch

Y = Radial distance from casing wall

δ = Boundary layer thickness

δ^* = Boundary layer displacement thickness

$\phi = \frac{\overline{C}_x}{U_m}$, flow coefficient

ρ = Density

ΔP_s = Increase in stagnation pressure between planes P.3 and P.4

ΔP_w = Increase in wall static pressure between planes P.3 and P.4

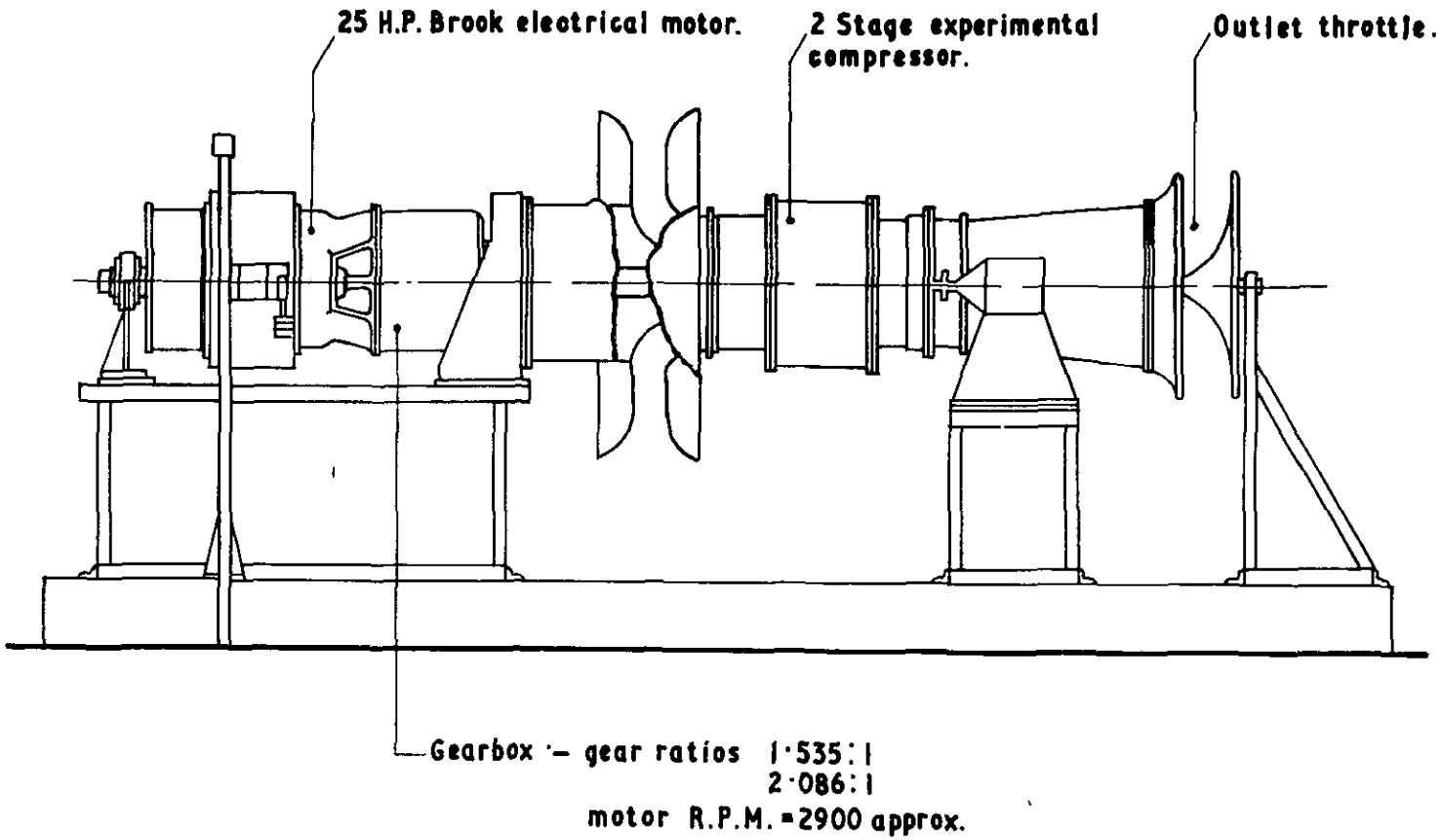

FIG.1. Experimental axial-flow compressor

Plane	
P.1	Airmeter static pressure tappings
P.2	Station used for fixing circular rings
P.3	Velocity profile traverses
P.4	Fixed reference hot-wire probe, stall patterns
P.5	Traversing hot-wire probe, stall patterns

Distance	Length
P.2 - P.3	1·90 in.
P.3 - P.4	2·10 in.
P.4 - P.5	1·90 in.

Annulus area:

Plane P.1 369·45 in.^{2}

Other planes 129·30 in.^{2}

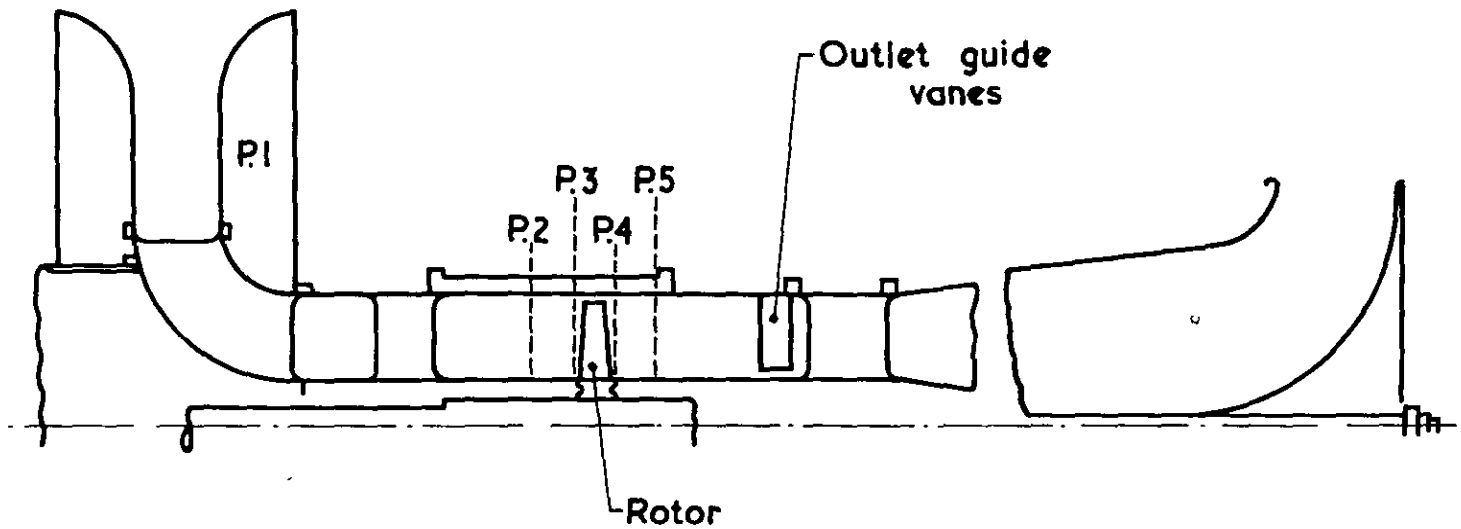

FIG.2. Compressor configuration

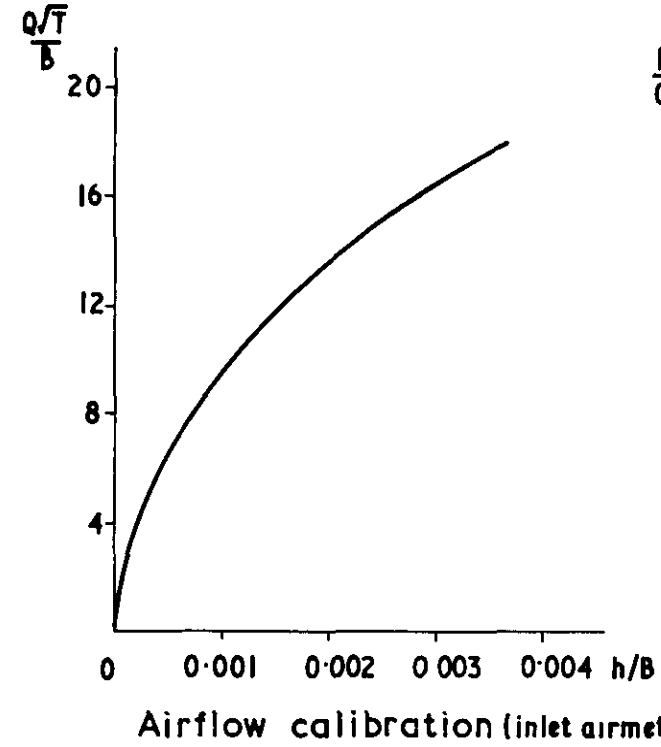

Airflow calibration (inlet airmeter)

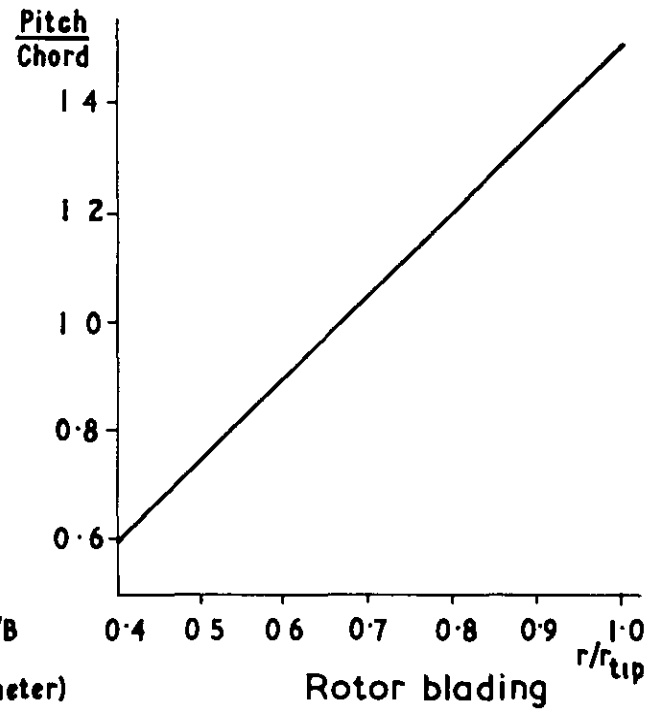

Rotor blading

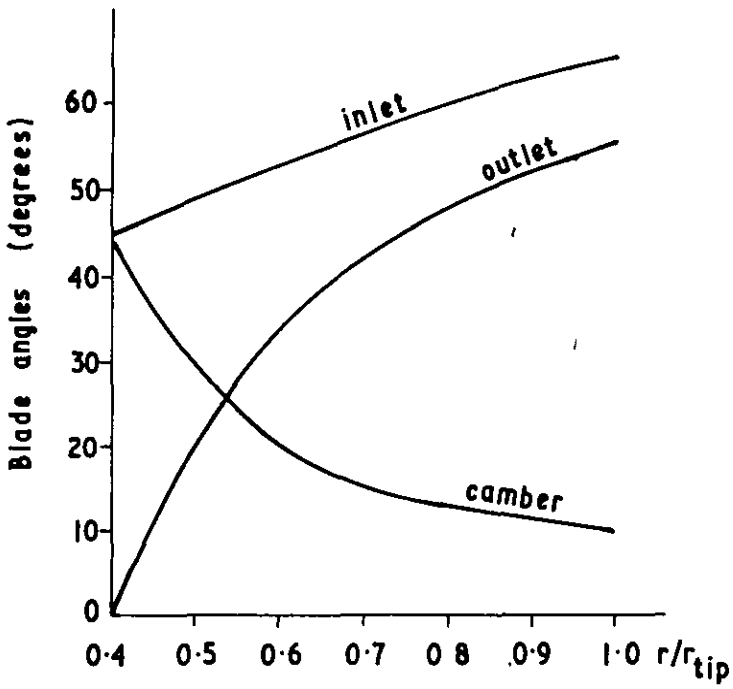

Rotor blading (angles)

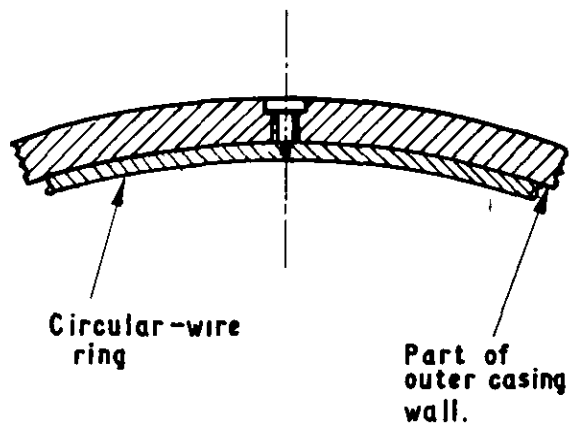

Circular-wire ring

FIG.3 Compressor components

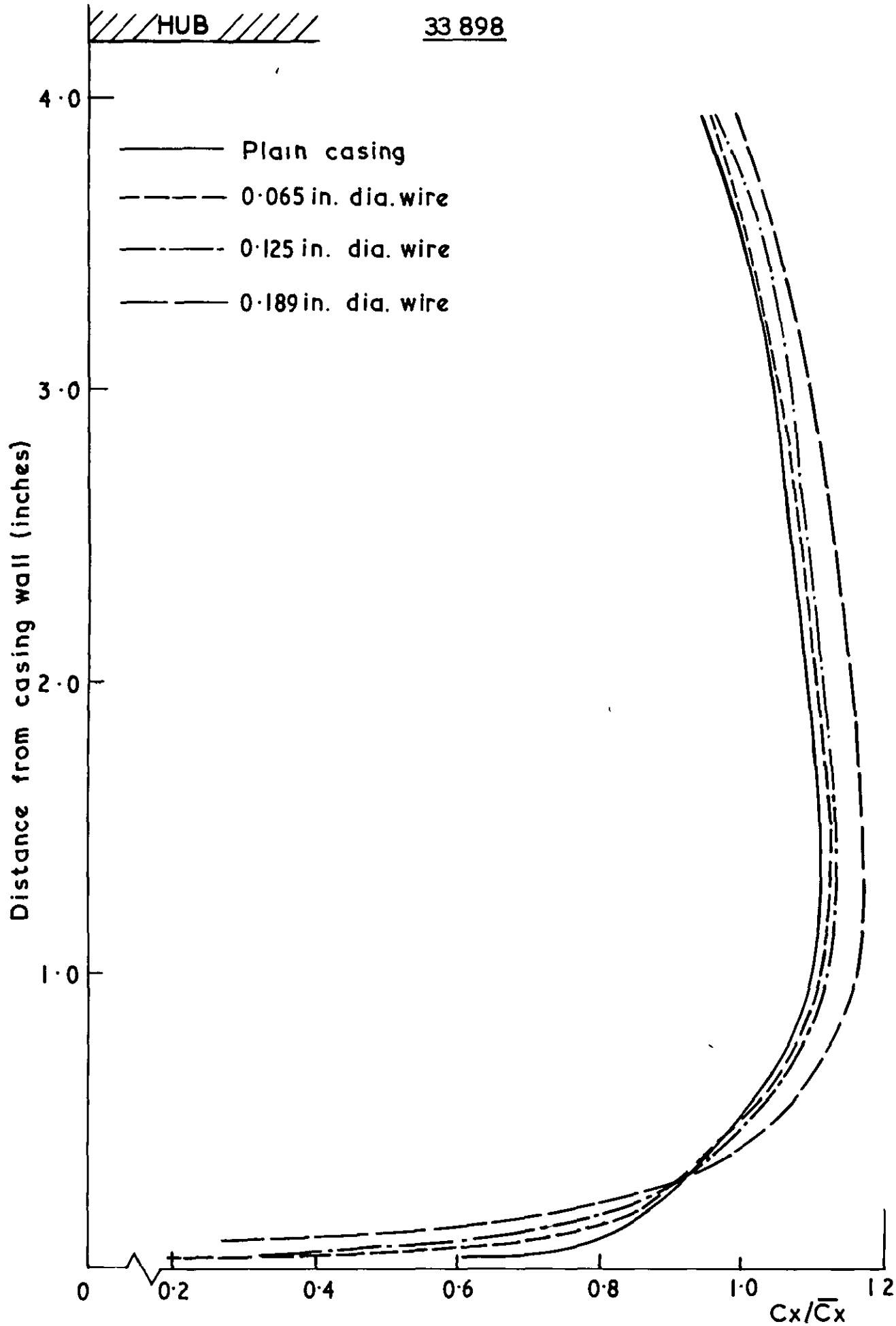

FIG.4. Upstream axial velocity profiles (prior to stall onset).

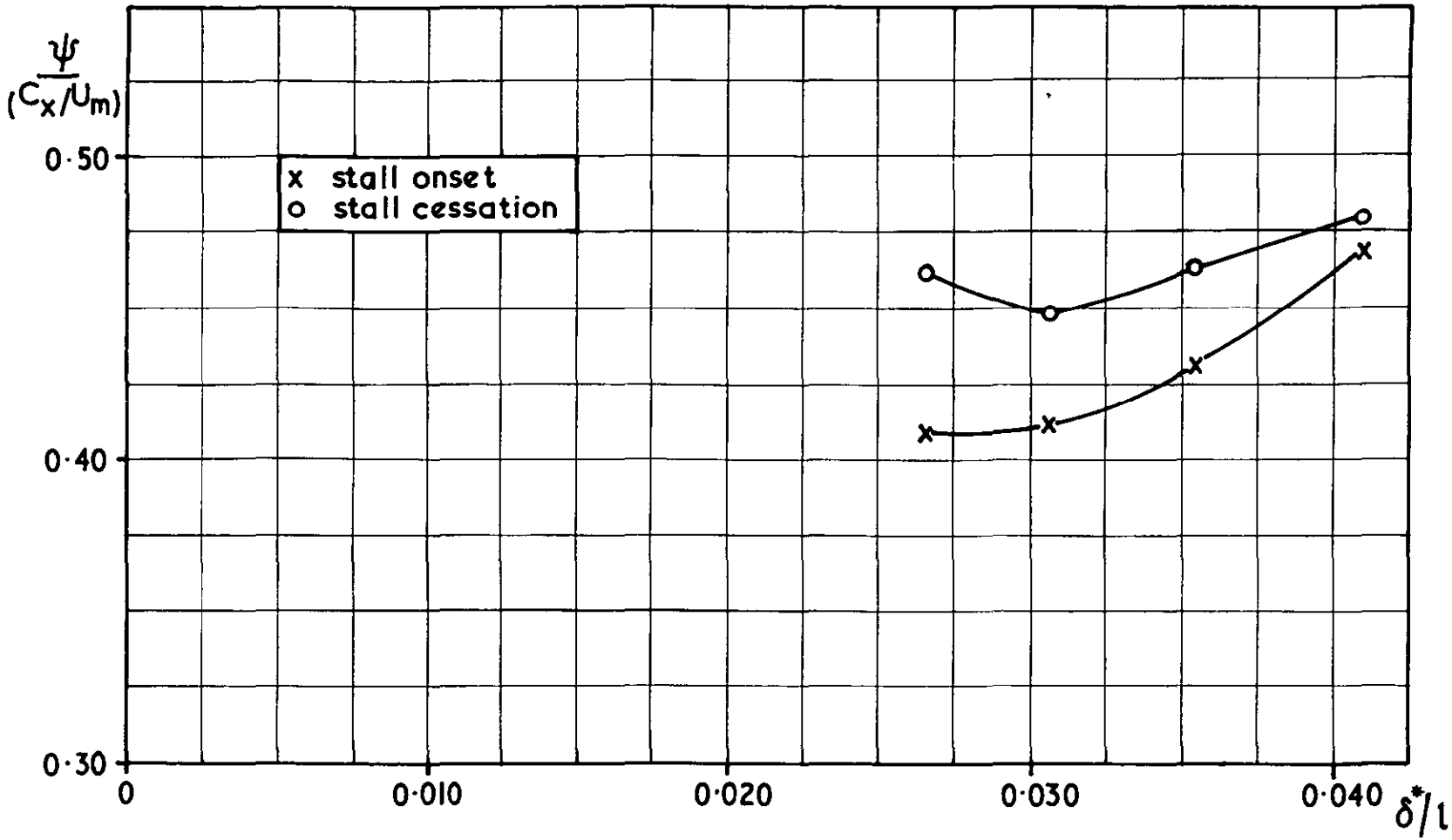

FIG.5. Effect of casing wall boundary layer on stall onset and cessation flow coefficients.

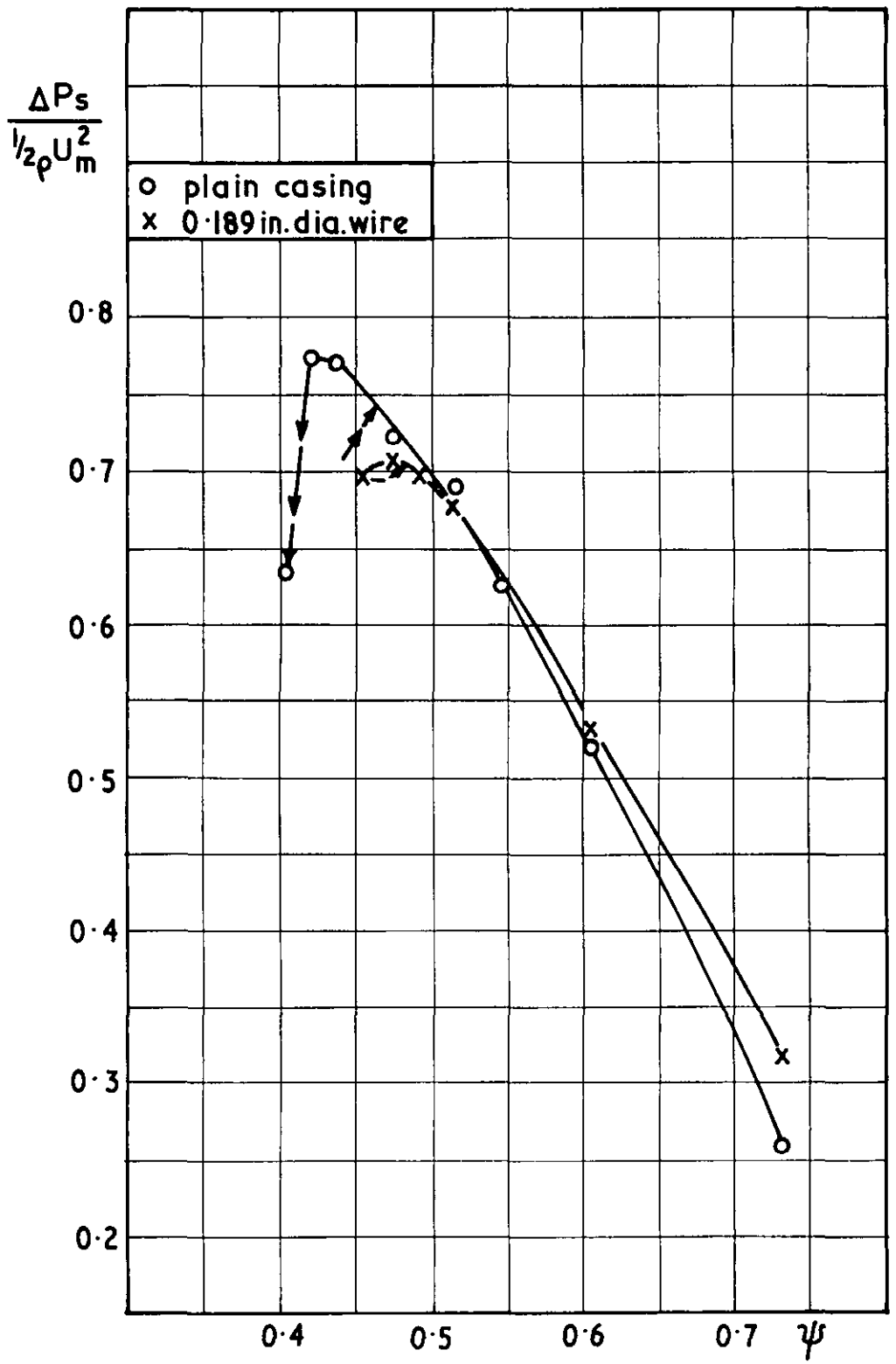

FIG. 6.(a) Non-dimensional characteristics.

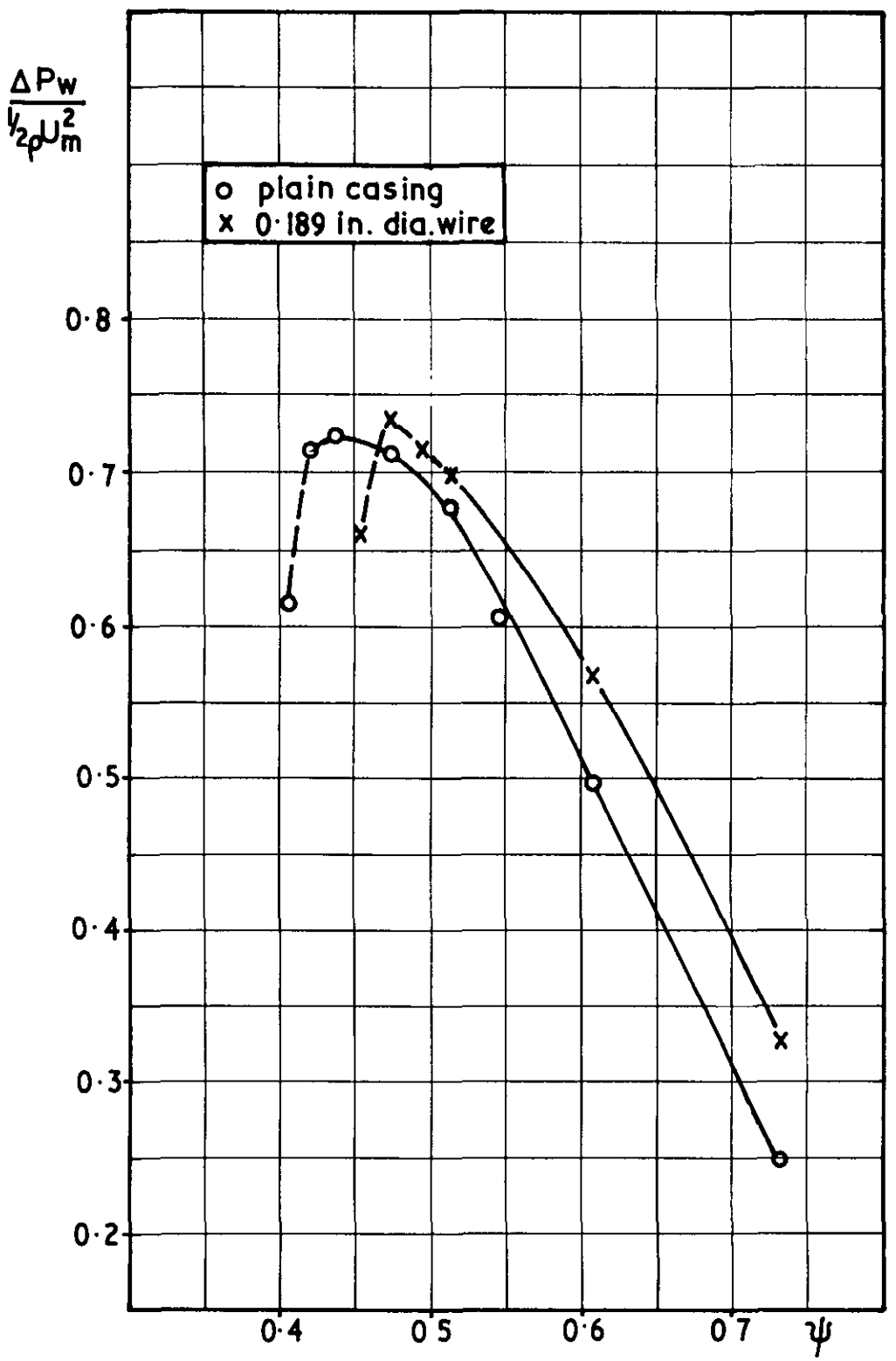

FIG. 6(b) Non-dimensional characteristics

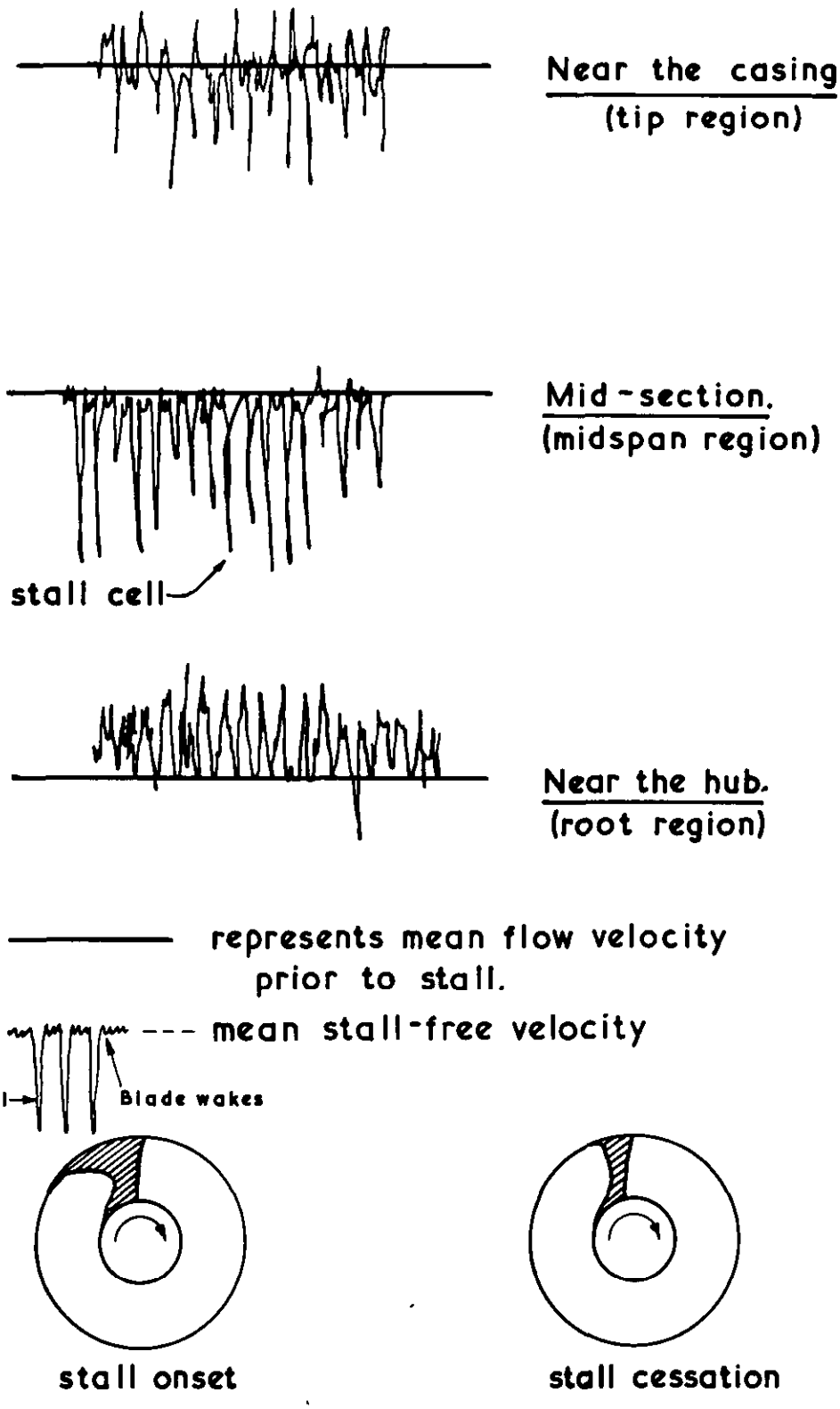

FIG.7. Stall patterns

HER MAJESTY'S STATIONERY OFFICE

Government Bookshops

49 High Holborn, London WC1V 6HB
13a Castle Street, Edinburgh EH2 3AR
109 St Mary Street, Cardiff CF1 1JW
Brazennose Street, Manchester M60 8AS
50 Fairfax Street, Bristol BS1 3DE
258 Broad Street, Birmingham B1 2HE
80 Chichester Street, Belfast BT1 4JY

Government publications are also available through booksellers

C.P. No. 1255

SBN 11 470813 4